Nanomaterials and Nanotechnology

OPEN ACCESS
ARTICLE

Polarimetric Detection of Enantioselective Adsorption by Chiral Au Nanoparticles – Effects of Temperature, Wavelength and Size

Invited Article

Nisha Shukla[2], Nathaniel Ondeck[1], Nathan Khosla[1], Steven Klara[1], Alexander Petti[1] and Andrew Gellman[1]*

1 Department of Chemical Engineering, Carnegie Mellon University, Pittsburgh, PA, USA
2 Institute of Complex Engineered Systems, Carnegie Mellon University, Pittsburgh, PA, USA
*Corresponding author(s) E-mail: gellman@cmu.edu

Received 01 November 2014; Accepted 07 January 2015

DOI: 10.5772/60109

Abstract

R- and *S*-propylene oxide (PO) have been shown to interact enantiospecifically with the chiral surfaces of Au nanoparticles (NPs) modified with *D*- or *L*-cysteine (cys). This enantiospecific interaction has been detected using optical polarimetry measurements made on solutions of the *D*- or *L*-cys modified Au (cys/Au) NPs during addition of racemic PO. The selective adsorption of one enantiomer of the PO onto the cys/Au NP surfaces results in a net rotation of light during addition of the racemic PO to the solution. In order to optimize the conditions used for making these measurements and to quantify enantiospecific adsorption onto chiral NPs, this work has measured the effect of temperature, wavelength and Au NP size on optical rotation by solutions containing *D*- or *L*-cys/Au NPs and racemic PO. Increasing temperature, decreasing wavelength and decreasing NP size result in larger optical rotations.

Keywords chiral, nanoparticle, enantioselective, adsorption, separation, Au

1. Introduction

The importance of chirality arises from the need of the pharmaceutical industry, and other producers of bioactive compounds, for chemical processes that are enantioselective and thereby produce enantiomerically pure chiral products. [1-4] This is one of the most challenging forms of chemical synthesis and is critical to the performance of bioactive chiral products. Ingestion of the two enantiomers of a chiral compound by a living organism can result in dramatically different physiological impacts, ranging from therapeutic for one enantiomer of a pharmaceutical to toxic for the other. Enantioselective chemical processing requires the use of enantiomerically pure chiral media. [5], [6] These could be enantiomerically pure chiral reagents, chiral homogeneous catalysts, chiral solvents, or chiral surfaces for adsorption or heterogeneous catalysis. Needless to say, chiral nanostructured materials have a role to play in enantioselective chemical processing technologies. [5], [7]

Over the past two decades, there has been enormous progress in the ability to synthesize nanoparticles (NPs)

with exquisite control over size, shape, morphology and function. [8-10] Most recently, there has been growing interest in and appreciation of the fact that some metal NPs can be chiral. [11-17] Although metals have achiral bulk structures, metal NPs can be chiral. The simplest form of chirality induction into a metal NP occurs by adsorption of a chiral ligand onto the NP surface. Such ligands render the surface chiral simply by creating a chiral environment at the surface, a process often called chiral templating. However, ligands can also imprint chirality onto the structure of the adsorbing NP by reconstructing its surface such that the metal atoms adopt a chiral structure. [18], [19] Alternatively, metallic NPs can expose surfaces with high Miller index facets, which are naturally chiral and, therefore, capable of enantiospecific adsorption. [1, 2, 7, 20-26] The key to giving any of these chiral NPs enantiospecific properties is that they are prepared in enantiomerically pure form, in some cases simply by modifying their surfaces with enantiomerically pure chiral ligands such as 2, 2′-bis(diphenylphosphino)-1, 1′-binaphthyl, [27] N-iosobutyryl-*L*-cysteine, [14] or penicillamines. [28] For the most part, previous work on chiral NPs has focused on their structure and on their optical properties, [11], [12], [28]-[31] however, attention has been focussed more recently on their enantiospecific interactions with chiral probe molecules. [32], [33] Ultimately, this effort will lead to enantioselective NP functionality in processes such as separations and catalysis.

This work furthers a methodology originally developed by the authors for the use of optical polarimetry measurements as a means of quantifying the enantiospecific interactions of chiral probe molecules with chiral Au NPs. [32], [33] The Au NPs are rendered chiral by modification of their surfaces with either *D*- or *L*-cysteine (cys). The key observation that reveals their enantioselectivity is that during the addition of racemic propylene oxide (rac-PO) to solutions containing either *D*- or *L*-cys/Au NPs there is a change in optical rotation of linearly polarized light. If the solution contains a racemic mixture of *D*- and *L*-cys/Au NPs, then the addition of rac-PO causes no rotation of light. The rotation of light by addition of rac-PO to solutions of enantiomerically pure Au NPs arises from two effects. One is the fact that the enantiomers of PO adsorb enantiospecifically to the chiral Au NPs because their adsorption equilibrium constants are enantiospecific: $K_{R/D} = K_{S/L} \neq K_{S/D} = K_{R/L}$, where $K_{R/D}$ is the adsorption equilibrium constant for *R*-PO on *D*-cys/Au NPs. As a result, the concentrations of the two enantiomers of PO in solution differ, and their concentrations in the adsorbed phase also differ. The second effect that induces optical rotation is that the specific optical rotation of the PO in solution differs from that of PO in the adsorbed phase: $-\alpha_R^{sol} = \alpha_S^{sol} \neq \alpha_S^{ads} = -\alpha_R^{ads}$, where α_S^{sol} is the specific optical rotation of *S*-PO in the solution phase. Thus, although the total amounts of each enantiomer of PO added to the solution as a racemic mixture are identical, their unequal partitioning between the solution phase and the adsorbed phase, coupled with the difference in optical rotation in the two phases yields a net optical rotation of light. This phenomenon can be described quite easily to yield a model that is parameterized by the four adsorption equilibrium constants and four specific optical rotation constants (four independent parameters in total). Given a sufficient number of measurements of optical rotation by solutions containing mixtures of *R*- and *S*-PO with *D*- and *L*-cys/Au NPs, it is possible to extract quantitative estimates of the ratios of the adsorption equilibrium constants: $\frac{K_{R/D}}{K_{R/L}} = \frac{K_{S/L}}{K_{S/D}}$. These ratios can be used to estimate the enantiospecific difference in the free energies of adsorption of PO on cys/Au: $\Delta\Delta G_{DL} = \Delta G_{R/D} - \Delta G_{R/L} = \Delta G_{S/L} - \Delta G_{S/D}$.

The use of optical rotation measurements as a means of quantifying enantiospecific adsorption constants relies on careful measurements of optical rotation in solutions with many different concentrations of chiral probe molecules and chiral NPs. Optical rotation will depend on the wavelength of the light being used for the measurements and on the concentrations of probe molecule enantiomers in the solution phase and adsorbed phase. In turn, the concentrations will depend on temperature through the temperature dependence of the adsorption equilibrium constants. The concentrations will depend on NP size through the net surface area for adsorption. In principle, the adsorption equilibrium constants could depend on NP size, although the size of the NPs used in this work have been quite large (4 - 80 nm) and a strong influence of NP size on the adsorption equilibrium constants seems unlikely. The influence of wavelength, temperature and NP size on optical rotation is complex, and so the empirical study described herein has been performed to explore their influence on optical rotation in order to guide future work towards choosing experimental parameters that will maximize measurement sensitivity and thereby optimize the quality of the resulting data.

2. Experimental

Au (III) chloride hydrate ($HAuCl_4\ xH_2O$, >99.9 %), trisodium citrate dihydrate ($C_6H_5Na_3O_7\ 2H_2O$, 99 %), sodium borohydride ($NaBH_4$, 99.9 %), *L*-cys ($C_3H_7NO_2S$, >97 %), *D*-cys ($C_3H_7NO_2S$, 99 %) and rac-cys ($C_3H_7NO_2S$, >97 %) were purchased from Sigma Aldrich and were used without further purification. *R*- and *S*-propylene oxide (C_3H_6O, 99 %) were purchased from Alfa Aesar.

2.1 Synthesis of chiral 4 nm Au NPs

The study of enantioselective separation at different temperatures and using different optical wavelengths was conducted with cys/Au NPs with diameters of ~4 nm synthesized as reported in earlier work. [32] A 20 mL aqueous (distilled water) solution of 2.5×10^{-4} M Au(III) chloride hydrate ($HAuCl_4\ xH_2O$) and 2.5×10^{-4} M trisodium citrate dihydrate ($C_6H_5Na_3O_7\ 2H_2O$) was prepared in a three-neck round bottom flask. After 10 minutes of vigo-

rous mixing using a magnetic stir plate, 0.6 mL of freshly prepared 0.1 M sodium borohydride ($NaBH_4$) was injected into the flask. The solution was shielded from light and was allowed to stir for 24 hours or until the colour changed from a bright red to a deep red or purple. This resulted in a solution of Au NPs. The Au NPs were modified by mixing 1 mL of the Au NP solution with 5 mL of 0.025 M cys in distilled water. The solution was sonicated for approximately 40 minutes and then allowed to sit for approximately two hours before making optical rotation measurements.

2.2 Synthesis of 50–80 nm Au NPs

The synthesis of variable-size Au NPs was adapted from a procedure published by Nasir *et al*. [34] The synthesis was performed in a three-neck flask covered in aluminium foil to eliminate light exposure and avoid degradation of the NPs. A 50 mL solution of (0.005 g) Au(III) chloride hydrate ($HAuCl_4\,xH_2O$) was prepared in deionized water in a round bottomed flask. The flask was heated to boiling with a reflux condenser while being continuously stirred. A 1% solution of trisodium citrate dihydrate ($C_6H_5Na_3O_7\ 2H_2O$) in deionized water was quickly added to the boiling solution. The volume added dictated the final size of the NPs. Adding volumes of 260 or 210 μL resulted in NPs with diameters of 50 or 80 nm, respectively, as determined by TEM and UV-vis. Once the trisodium citrate dihydrate ($C_6H_5Na_3O_7\ 2H_2O$) was added, the colour of the synthesis mixture began to change from yellow/clear to black and then to red (for smaller particles) or purple (for larger particles). The colour change occurs within a few seconds and after the colour change stopped, the solution was refluxed for an additional 10 minutes. The solution was then removed from the heat source, and continuously stirred until it reached room temperature. The solution was then stored in the dark where it remained stable for several days.

2.3 Optical rotation measurements

All optical rotation measurements were made with a Rudolph Research Analytical Autopol VI polarimeter using a TempTrol Hastelloy measurement cell. In order to allow the cell to reach the desired temperature, sample solutions were allowed to sit in the cell mounted in the polarimeter for 10 minutes prior to making measurements. Measurements of optical rotation were made using wavelengths of 365, 436 and 546 nm with temperatures of 23, 30 and 40 °C. Ten measurements of optical rotation were made at each of these conditions. The data reported in this paper are measurements of optical rotation angle versus concentration of *R*-, *S*-, or rac-PO and quantified as the slopes of these data in units of °/M, all of which were measured in the linear regime of their dependence on concentration. Although these measurements do not allow an absolute determination of the coverage of PO on the cys/Au NPs, the linear regime suggests that the coverages are low relative to the saturated monolayer. Each reported value of the optical rotation is the average of 10 measurements. The uncertainties reported for the slopes are the uncertainties propagated from the scatter of the data around the best fit line.

After the 6 ml cys/Au NP solution sat for two hours following sonication, a 2 ml aliquot was injected into the TempTrol Hastelloy measurement cell and placed into the Rudolph Autopol VI. The instrument was programmed to wait for 10 minutes and then record 10 consecutive measurements of optical rotation and report the average of these values. Immediately after the program was started, the desired amount of rac-PO was mixed with the remaining 4 ml of cys/Au NP solution and briskly shaken. After the 10 minute time delay and 10 consecutive measurements of optical rotation, the 2 ml sample in the TempTrol Hastelloy measurement cell was added to the 4 ml solution of chiral cys/Au NPs with rac-PO and thoroughly mixed. From that solution a 2 ml aliquot was removed and placed in the TempTrol cell to start the next set of optical rotation measurements. Additional rac-PO was then added to the remaining 4 ml of solution, and the entire process repeated until the maximum desired PO concentration was reached.

The Rudolph Research Analytical Autopol VI has the ability to switch between six wavelengths and to control the temperature of the sample in the TempTrol Hastelloy measurement cell. This work used wavelengths of 365, 436 and 546 nm and temperatures of 23, 30 and 40 °C.

3. Results and discussion

Following the procedures developed and described in our previous studies of optical rotation by solutions of PO and chiral cys/Au NPs, [32], [33] this study has measured the optical rotation of solutions prepared by adding rac-PO in increasing concentrations to solutions containing *D*- or *L*-cys/Au NPs. The *D*- and *L*-cys/Au NP solutions (without PO) rotate linearly polarized light as a result of the chirality of the cys/Au NPs and the residual *D*- or *L*-cys in the solution phase. If there were no enantiospecific interactions between the enantiomers of PO and the *D*- or *L*-cys/Au NPs, the addition of a rac-PO would not result in any change in optical rotation. Note that the detectable interactions between the enantiomers of PO and the *D*- or *L*-cys in solution are weak with respect to those between PO and *D*- or *L*-cys/Au NPs. [32] The goal of this work has been an empirical study of the effects of light wavelength, temperature and NP size on the degree of optical rotation observed in these types of experiments. This will guide the choice of conditions used for future quantitative measurements of the enantiospecific equilibrium constants for adsorption of chiral probe molecules on chiral NPs.

3.1 Wavelength dependence of optical rotation by rac-PO in cys/Au NP

The effect of wavelength on optical rotation was observed during addition of rac-PO to solutions containing chiral and achiral cys/Au NPs with diameters of ~4 nm. Figure 1 shows the effect of wavelength on optical rotation of light by solutions of *D*- or *L*-cys/Au NPs measured as a function

of rac-PO concentration and at 23 °C. The specific optical rotation constants are wavelength dependent, [35], [36] and would influence the sensitivity of the measurements, if there is a difference in the wavelength dependences of the optical rotation constants for PO in the solution phase, α^{sol}, and in the adsorbed phase, α^{ads}. The chirality of the *D*- or *L*-cys/Au NPs is evident from the fact that they rotate light prior to the addition of rac-PO (Figure 1). The magnitude of optical rotation increases from 0.1° to 0.2° as the wavelength is decreased from 546 to 365 nm. The enantiospecific interactions of the *R*- and *S*-PO with the *D*- or the *L*-cys/Au NPs are evident from the increase in the optical rotation by addition of rac-PO to the solutions. The slopes of the curves are indicated at the left side of the plot in Figure 1 and increase by a factor of ~3 as the wavelength is decreased from 546 to 365 nm. The variance in the measured slopes seems to increase more slowly than the magnitude of the slope indicating that the shorter wavelengths are slightly better suited to giving higher accuracy measurements.

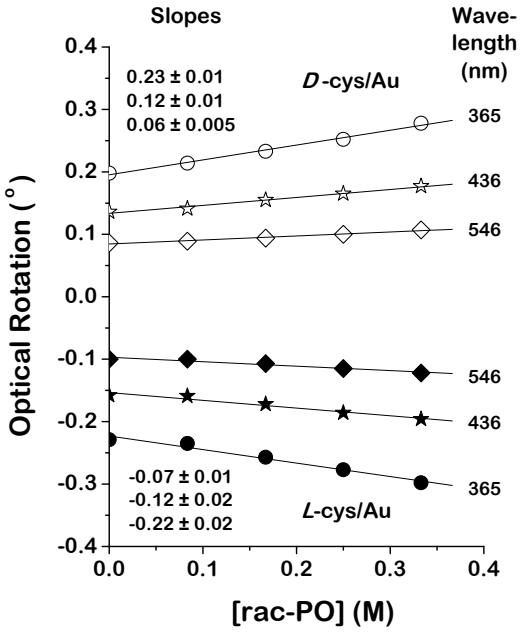

Figure 1. Optical rotation of linearly polarized light at wavelengths of λ = 546, 436 and 365 nm during addition of rac-PO to solutions containing *D*- or *L*-cys/Au NPs. Quantities at left are the slopes of rotation angle versus PO concentration. Measurements made at: T = 23 °C, NP diameter ~4 nm, [Au] = 1.6×10^{-5} g/mL, [cys] = 0.025 M, pH = 8.

A set of measurements of optical rotation by *R*-, *S*-, or rac-PO in solution with *D*-cys/Au, *L*-cys/Au, rac-cys/Au or bare Au NPs have been made using 365 nm light and a temperature of 23 °C. These are comparable to experiments reported earlier using 436 nm light and room temperature, without temperature control. [32] As shown in Figure 2, the specific rotation of *R*- and *S*-PO at 365 nm has a value of $|\alpha^{sol}|$ = 1.45 °/M which is about 70 % higher than that measured previously using 465 nm light. Equally important, the temperature control reduces the uncertainty in these measurements by a factor of 2. The measurements of optical rotation by pure *R*- or *S*-PO in the presence of bare Au NPs and rac-cys/Au NPs (Figure 2) shows the enhancement of optical rotation that arises from adsorption of the PO on the NPs. These show smaller enhancements of optical rotation with respect to measurements at 436 nm than in the case of pure *R*- or *S*-PO but significant reduction in the uncertainty of the slopes. Enantiospecific interactions of the *R*- and *S*-PO with *D*- or *L*-cys/Au NPs are revealed by the optical rotation measurements in Figure 3. The magnitudes of the optical rotations of *R*- and *S*-PO are enhanced with respect to the solution phase. More importantly, for *S*-PO the rotation is greater in the presence of *D*-cys/Au than in the presence of *L*-cys/Au. Consistent with a diastereomeric relationship, the opposite is true for *R*-PO. This is demonstrated more convincingly in these measurements at 365 nm than in prior work at 436 nm. Finally, Figure 4 shows the rotation of light during addition of rac-PO to solutions containing *D*-cys, *L*-cys, rac-cys/Au, *D*-cys/Au or *L*-cys/Au NPs. The first three are control experiments. The solutions containing either *D*- or *L*-cys (0.025 M) are chiral and rotate light. However, they exhibit relatively weak enantiospecific interactions with PO; the addition of rac-PO results in small changes in the optical rotation relative to the rotations observed in the presence of *D*- or *L*-cys/Au NPs. The rac-cys/Au NPs are not chiral, do not rotate light and, not surprisingly, the addition of rac-PO to the solution does not cause any rotation of light. The key point is that the addition of rac-PO to the solutions containing either *D*- or *L*-cys/Au NPs results in a net rotation of light. These data obtained at 365 nm exhibit the enhanced optical rotation of ~90 % over that obtained at 436 nm as shown in Figure 1.

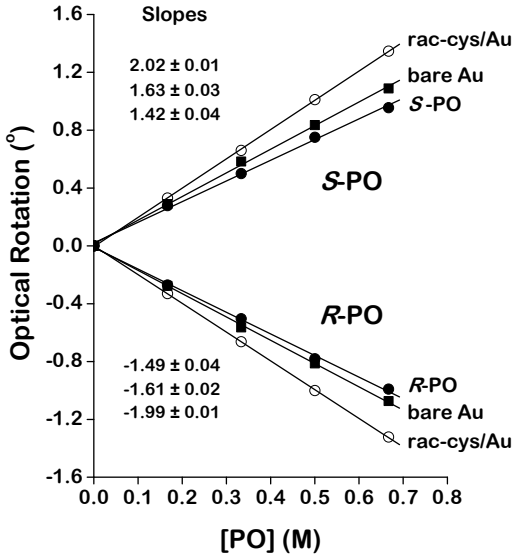

Figure 2. Rotation of light versus [PO] by enantiomerically pure *R*- and *S*-PO in aqueous solution with and without bare Au and rac-Au NPs. In water (●) the *R*- and *S*-PO rotate light by equal and opposite angles with a specific rotation of ~1.4 °/M. In the presence of bare Au NPs (■) and rac-cys/Au NPs (○) the specific rotation is measurably increased. Measurements made at: λ = 365 nm, T = 23 °C, NP diameter ~4 nm, [Au] = 1.6×10^{-5} g/mL, [cys] = 0.025 M, pH = 8.

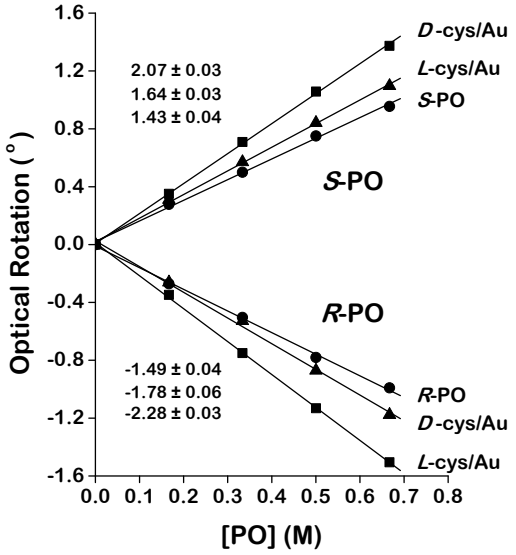

Figure 3. Optical rotation versus *R*- and *S*-PO concentration in aqueous solutions (●) and in solutions containing *D*- or *L*-cys/Au NPs. The data from the solutions containing the heterochiral pairs (*R*-PO/*L*-cys/Au and *S*-PO/*D*-cys/Au) are marked with solid squares (■). The data from solutions containing the homochiral pairs (*R*-PO/*D*-cys/Au and *S*-PO/*L*-cys/Au) are marked with solid triangles (▲). The differences between the homochiral and the heterochiral pairs are indicative of the enantiospecific interaction of *R*- and *S*-PO with the chiral Au NPs. Measurements made at: λ = 365 nm, T = 23 °C, NP diameter ~4 nm, [Au] = 1.6×10^{-5} g/mL, [cys] = 0.025 M, pH = 8.

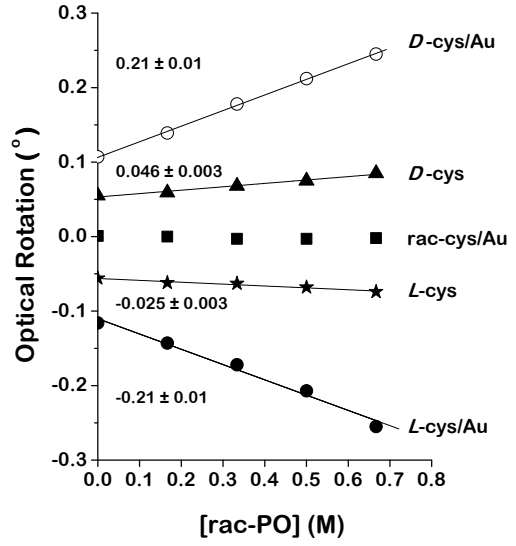

Figure 4. Rotation of polarized light versus rac-PO concentration in solutions containing: rac-cys/Au NPs (■), *L*- or *D*-cys (⋆, ▲), and *L*- or *D*-cys/Au NPs (●, ○). The control measurements show that there are no enantiospecific interactions between PO and *L*-cys (⋆), *D*-cys (▲) or rac-cys/Au NPs (■). PO does interact enantiospecifically with *L*- and *D*-cys/Au NPs (●, ○), thus causing increased rotation of polarized light with increasing [rac-PO]. Measurements made at: λ = 365 nm, T = 23 °C, NP diameter ~4 nm, [Au] = 1.6×10^{-5} g/mL, [cys] = 0.025 M, pH = 8.

3.2 Temperature dependence of optical rotation by rac-PO in cys/Au NPs

The next experiment studied the effect of temperature on enantioselective partitioning of rac-PO on cys/Au NPs. Temperature influences the system through the enantiospecific adsorption equilibrium constants, $K_{R/D}$ (and others). In principle, measuring the ratios of the adsorption equilibrium constants, $\frac{K_{R/D}}{K_{S/D}}$, over a range of temperatures allows direct determination of the enantiospecific heat and entropy of adsorption, $\Delta\Delta H_{R\text{-}S}$ and $\Delta\Delta S_{R\text{-}S}$, respectively; although the limited temperature range may make this difficult. Figure 5 shows measurements of optical rotation by rac-PO in *D*-cys/Au NPs at 23, 30 and 40 °C and under temperature control. The size of the cys/Au NPs was 4 nm and the solution pH = 8. In our previous work [32, 33] all experiments were performed at room temperature without temperature control. The optical rotation by the *D*-cys/Au NPs alone shows slight but not significant temperature dependence; however, the slopes of the optical rotation with respect to rac-PO concentration double over the temperature range of 23 to 40 °C. The origin of this effect is the temperature dependence of the ratios of the enantiospecific adsorption equilibrium constants, $\frac{K_{R/D}}{K_{S/D}}$.

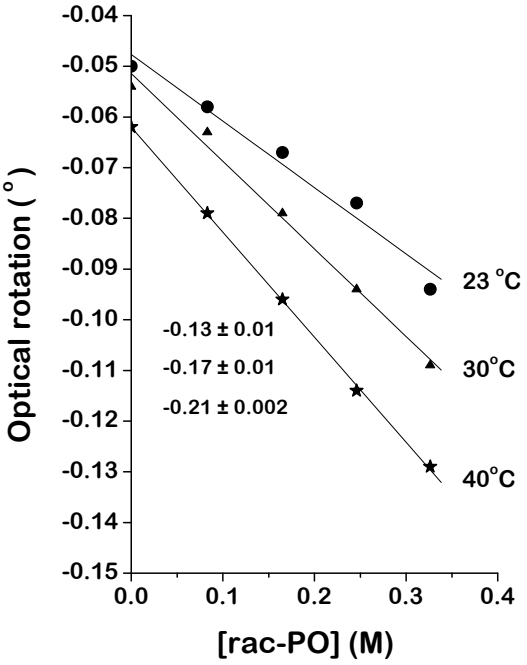

Figure 5. Optical rotation versus concentration of rac-PO in solutions containing *D*-cys/Au NPs at temperatures of 23, 30 and 40 °C. Slopes of the data are given in the left side of the graph. Measurements made at: λ = 436 nm, NP diameter ~4 nm, [Au] = 1.6×10^{-5} g/mL, [cys] = 0.025 M, pH = 8.

A set of measurements of optical rotation by *R*-, *S*-, or rac-PO in solution with *D*-cys/Au, *L*-cys/Au, rac-cys/Au or bare Au NPs have been made at 40 °C and a wavelength of 436 nm (Figures 6–8). These are comparable to experiments reported earlier using 436 nm light and room temperature, without temperature control (Table 1). [32] The magnitude of the specific optical rotation by *R*- and *S*-PO in solution is $|\alpha^{sol}|$ = 0.80 °/M, which is ~10 % lower than that reported earlier, and is not surprising as the optical rotation constants themselves should not be very temperature depend-

ent in molecules that have only one conformation. [35] The measurements in solutions containing bare Au or rac-cys/Au NPs (Figure 6) reveal the enhancement of optical rotation that arises from adsorption on the Au NPs. However, the magnitudes of the slopes are now ~50 % lower than the values reported at room temperature. [32] This suggests that the increased temperature has resulted in a decrease in the adsorption equilibrium constants, consistent with an exothermic heat of adsorption. As in Figure 3, the data in Figure 7 showing the rotation of light for *R*- or *S*-PO in solution with either *D*- or *L*-cys/Au NPs reveal a diastereomeric relationship between the four measurements, and clearly reveal an enantiospecific interaction of PO with cys/Au NPs. Finally, the addition of rac-PO to solutions containing *D*-cys, *L*-cys, rac-cys/Au, *D*-cys/Au or *L*-cys/Au NPs induces the optical rotation shown in Figure 8. The control experiments using *D*-cys, *L*-cys, and rac-cys/Au showed no net change in optical rotation as a result of adding the rac-PO. On the other hand, the net rotation induced by addition of rac-PO to solutions containing the *D*- or *L*-cys/Au NPs clearly reveals enantiospecific adsorption on the NPs. The optical rotation measured of 0.23 °/M at 40 °C is significantly higher than the value of 0.15 °/M reported earlier from measurements made at room temperature. [32]

Measurement conditions		rac-PO on	rac-PO on
Temp (°C)	λ (nm)	*L-cys/Au*	*D-cys/Au*
23	436	-0.15±0.01	0.15±0.01
23	365	-0.21±0.01	0.22±0.01
40	365	-0.20±0.01	0.25±0.01

Table 1. Slope of optical rotations versus rac-PO concentration for solutions with *L*- or *D*-cys/Au NPs at different wavelengths and temperatures

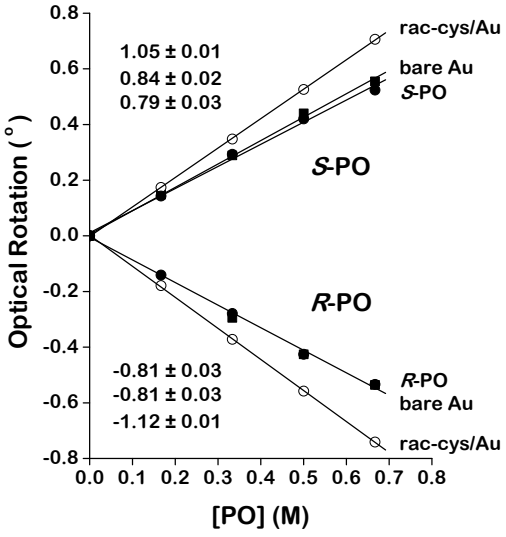

Figure 6. Rotation of light versus concentration of enantiomerically pure *R*- or *S*-PO in aqueous solution, with bare Au NPs and with rac-cys/Au NPs. When dissolved in water (●) the *R*- and *S*-PO rotate light by equal and opposite angles with a specific rotation of 1.1 °/M. In the presence of bare Au NPs (■) and rac-cys/Au NPs the specific rotation is increased measurably. Measurements made at: λ = 436 nm, T = 40 °C, NP diameter ~4 nm, [Au] = 1.6×10^{-5} g/mL, [cys] = 0.025 M, pH = 8.

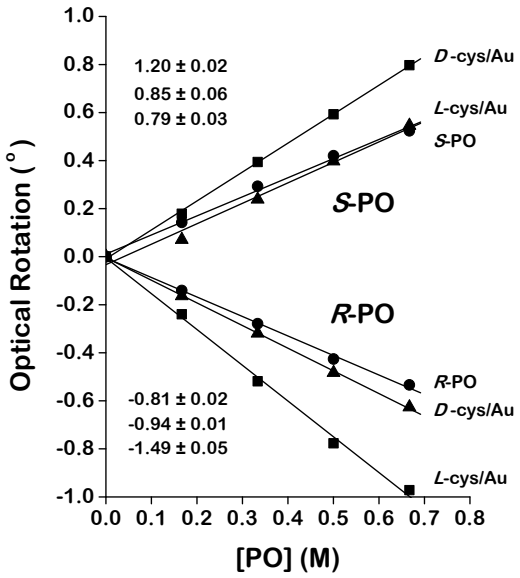

Figure 7. Optical rotation versus concentration of *R*- and *S*-PO in aqueous solution (●) and in solutions containing *D*- or *L*-cys/Au NPs. The data from the solutions containing the heterochiral pairs (*R*-PO/*L*-cys/Au and *S*-PO/*D*-cys/Au) are marked with solid squares (■). The data from solutions containing the homochiral pairs (*R*-PO/*D*-cys/Au and *S*-PO/*L*-cys/Au) are marked with solid triangles (▲). The differences of the homochiral and the heterochiral pairs are indicative of the enantiospecific interaction of *R*- and *S*-PO with the chiral Au NPs. Measurements made at: λ = 436 nm, T = 40 °C, NP diameter ~4 nm, [Au] = 1.6×10^{-5} g/mL, [cys] = 0.025 M, pH = 8.

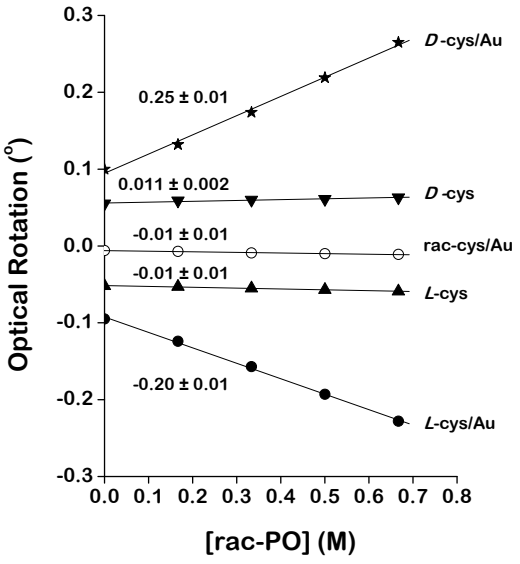

Figure 8. Rotation of polarized light versus concentration of rac-PO added to solutions containing: rac-cys/Au NPs (○), *L*- or *D*-cys (▲, ▼), or *D*- or *L*-cys/Au NPs (⋆, ●). The control measurements show that there are no enantiospecific interactions between PO and *L*-cys, *D*-cys or rac-cys/Au NPs. PO interacts enantiospecifically with *D*- or *L*-cys/Au NPs, thus causing increased rotation of polarized light with increasing [rac-PO]. Measurements made at: λ = 436 nm, T = 40 °C, NP diameter ~4 nm, [Au] = 1.6×10^{-5} g/mL, [cys] = 0.025 M, pH = 8.

3.3 NP size effects on optical rotation measurements

The optical rotation measurements used in this study can be influenced by NP size via three mechanisms. One is

simply a reduction in the surface area for PO adsorption. The other is an NP size effect on the specific optical rotation of light by adsorbed PO. The third is the size dependence of the enantiospecific adsorption equilibrium constants. The study of NP size effects has been performed by adding rac-PO to solutions of *D*- or *L*-cys/Au NPs with sizes of ~4, ~50, or ~80 nm. Measurements were made at 23 °C using 436 nm light. The increase in NP diameter results in a 400-fold decrease in the adsorbing surface area. The data in Figure 9 certainly reveal a decrease in the net rotation of light by addition of rac-PO to solutions containing NPs of different diameter; however, the net optical rotation is far from linearly proportional to the surface area of the NPs. For the larger particles with mean diameters of 80 and 50 nm, the surface area increases by ~2.5 for the smaller particles which is roughly consistent with the increase in the slopes of the optical rotations. However, the increase in the slopes of the optical rotation when going from 50 to 4 nm is only an additional 50 %. Recently, we have developed a measurement and analysis protocol that allows measurement of the ratios of the enantiospecific adsorption equilibrium constants without the need for direct determination of the NP surface area. [33] The interesting implication of the data in Figure 9 is that the optical rotation measurements have the sensitivity to allow study of enantiospecific adsorption across a wide range of NP sizes.

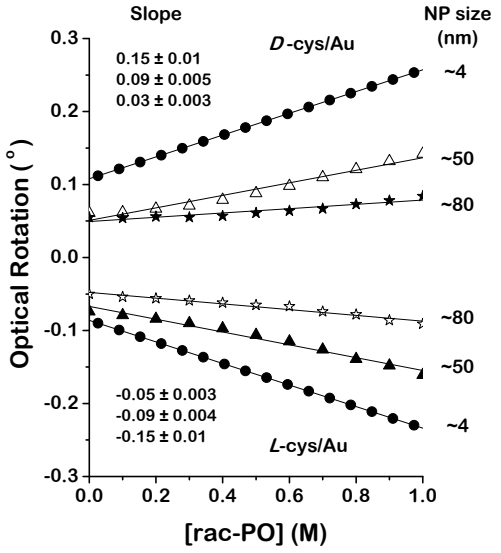

Figure 9. Rotation of polarized light versus concentration of rac-PO to solutions containing *D*- or *L*-cys/Au NPs with diameters of ~4, ~50, ~80 nm. The slopes of each data sets are at the left. Measurements made at: λ = 436 nm, T = 23 °C, [Au ~4 nm] = 1.6×10^{-5} g/mL, [Au ~50 nm and ~80 nm] = 1.4×10^{-5} g/mL, [cys] = 0.025 M, pH = 7.

4. Conclusions

The systematic study reported herein has demonstrated that optical wavelength, temperature and NP size influence the magnitudes of optical rotation measurements used for determination of the enantiospecific adsorption equilibrium constants for chiral probe molecules on chiral Au NPs. Increasing temperature while decreasing wavelength and NP size will enhance the sensitivity of these types of measurement. In the system being used for these studies, a wavelength of 365 nm and temperature of 40 °C will provide a ~50 % increase in optical rotation during addition of rac-PO to solutions containing chiral Au NPs. However, from the point of view of improved measurement accuracy, the ability to control temperature during extended sets of measurements appears to be equally important to improving measurement accuracy.

5. Acknowledgements

This work has been supported by the DOE through grant number DE-FG02-12ER16330. NS would like to acknowledge support from the Pennsylvania Infrastructure Technology Alliance.

6. References

[1] Gellman A J (2010) Chiral surfaces: Accomplishments and challenges. ACS Nano 4: 5-10.

[2] Sholl D S and Gellman A J (2009) Developing chiral surfaces for enantioselective chemical processing. AIChE Journal 55: 2484-2490.

[3] Stinson S C (2001) Chiral pharmaceuticals. Chemical and Engineering News 79 (40): 79–97

[4] Thayer A M (2007) Centering on chirality. Chemical and Engineering News 85: 11-19.

[5] Chang C L, Wang X, Bai Y and Liu H W (2012) Applications of nanomaterials in enantioseparation and related techniques. Trends Anal. Chem. 39: 195-206.

[6] Mallat T, Orglmeister E and Baiker A (2007) Asymmetric catalysis at chiral metal surfaces. Chemical Reviews 107: 4863-4890.

[7] Gellman A J and Shukla N (2009) Nanocatalysis - More than speed. Nature Materials 8: 87-88.

[8] Cuenya B R (2010) Synthesis and catalytic properties of metal nanoparticles: Size shape support composition and oxidation state effects. Thin Solid Films 518: 3127-3150.

[9] Grzelczak M, Perez-Juste J, Mulvaney P and Liz-Marzan L M (2008) Shape control in gold nanoparticle synthesis. Chemical Society Reviews 37: 1783-1791.

[10] Somorjai G A and Park J Y (2008) Colloid science of metal nanoparticle catalysts in 2D and 3D structures. Challenges of nucleation growth composition particle shape size control and their influence on activity and selectivity. Topics in Catalysis 49: 126-135.

[11] Li T H, Park H G, Lee H S and Choi S H (2004) Circular dichroism study of chiral biomolecules conjugated nanoparticles. Nanotechnology 15: S660-S663.

[12] Canfield B K et al (2006) Linear and nonlinear optical properties of gold nanoparticles with broken symmetry. Journal of Nonlinear Optical Physics and Materials 15: 43-53.

[13] Gautier C et al (2006) Probing chiral nanoparticles and surfaces by infrared spectroscopy. Chimia 60: A777-A782.

[14] Gautier C and Burgi T (2006) Chiral N-isobutyryl-cysteine protected gold nanoparticles: Preparation size selection and optical activity in the UV-vis and infrared. Journal of the American Chemical Society 128: 11079-11087.

[15] Shemer G et al (2006) Chirality of silver nanoparticles synthesized on DNA. Journal of the American Chemical Society 128: 11006-11007.

[16] Gautier C and Buergi T (2008) Chiral metal surfaces and nanoparticles. Chimia 62: 465-470.

[17] Gautier C and Burgi T (2009) Chiral gold nanoparticles. Chemphyschem 10: 483-492.

[18] Wu Z W, Gayathri C, Gil R R and Jin R C (2009) Probing the structure and charge state of glutathione-capped Au-25(SG)(18) Clusters by NMR and mass spectrometry. Journal of the American Chemical Society 131: 6535-6542.

[19] Jadzinsky P D, Calero G, Ackerson C J, Bushnell D A and Kornberg R D (2007) Structure of a thiol monolayer-protected gold nanoparticle at 1.1 angstrom resolution. Science 318: 430-433.

[20] McFadden C F, Cremer P S and Gellman A J (1996) Adsorption of chiral alcohols on "chiral" metal surfaces. Langmuir 12: 2483-2487.

[21] Quan Z, Wang Y and Fang J (2013) High-index faceted noble metal nanocrystals. Accounts of Chemical Research 46: 191-202.

[22] Yun Y, Wei D, Sholl D S and Gellman A J (2014) Equilibrium adsorption of D- and L-alanine mixtures on naturally chiral Cu{3 1 17}RandS surfaces. Journal of Physical Chemistry C 118: 14957-14966.

[23] Yun Y, Gellman AJ (2013) Enantioselective Separation on Naturally Chiral Metal Surfaces: d,l-Aspartic Acid on Cu(3,1,17)(R&S) Surfaces. Angew. Chem. Int. Edit. 52: 3394-3397.

[24] Horvath J D and Gellman A J (2001) Enantiospecific desorption of R- and S-propylene oxide from a chiral Cu(643) surface. Journal of the American Chemical Society 123: 7953-7954.

[25] Horvath J D and Gellman A J (2002) Enantiospecific desorption of chiral compounds from chiral Cu(643) and achiral Cu(111) surfaces. Journal of the American Chemical Society 124: 2384-2392.

[26] Horvath J D, Koritnik A, Kamakoti P, Sholl D S and Gellman A J (2004) Enantioselective separation on a naturally chiral surface. Journal of the American Chemical Society 12:6 14988-14994.

[27] Tamura M and Fujihara H (2003) Chiral bisphosphine BINAP-stabilized gold and palladium nanoparticles with small size and their palladium nanoparticle-catalyzed asymmetric reaction. Journal of the American Chemical Society 125: 15742-15743.

[28] Yao H, Miki K, Nishida N, Sasaki A and Kimura K (2005) Large optical activity of gold nanocluster enantiomers induced by a pair of optically active penicillamines. Journal of the American Chemical Society 127: 15536-15543.

[29] Yao H (2008) Optically active gold nanoclusters. Curr. Nanosci. 4: 92-97.

[30] Hidalgo F, Sanchez-Castillo A, Garzon I L and Noguez C (2009) First-principles calculations of circular dichroism of ligand-protected gold nanoparticles. European Physical Journal D 52: 179-182.

[31] Noguez C and Garzon I L (2009) Optically active metal nanoparticles. Chemical Society Reviews 38: 757-771.

[32] Shukla N, Bartel M A and Gellman A J (2010) Enantioselective separation on chiral Au nanoparticles. Journal of the American Chemical Society 132: 8575-8580.

[33] Shukla N, Ondeck N and Gellman A J (2014) Quantitation of enantiospecific adsorption on chiral nanoparticles from optical rotation. Surface Science 629: 15-19.

[34] Nasir S M and Nur H (2008) Gold nanoparticles embedded on the surfaces of polyvinyl alcohol layer. Malaysian Journal of Fundamental Science 4: 245-252.

[35] Wiberg K B, Wang Y G, Murphy M J and Vaccaro P H (2004) Temperature dependence of optical rotation: Alpha-pinene beta-pinene pinane camphene camphor and fenchone. Journal of Physical Chemistry A 108: 5559-5563.

[36] Ioan S, Cosutchi A I and Dorohoi D-O (2008) Optical rotatory dispersion for polymers. Romanian Journal of Physics 53: 85-90.